

The formation of internal bores in the atmosphere: A laboratory model

By JAMES W. ROTTMAN* and JOHN E. SIMPSON

Department of Applied Mathematics and Theoretical Physics, University of Cambridge

(Received 20 June 1988; revised 11 January 1989)

SUMMARY

Recently several atmospheric observations have been interpreted as internal undular bores or internal solitary waves evolving from internal bores that propagate along low-level temperature inversions. It has been speculated that such disturbances are generated by some type of gravity current (such as cold fronts, sea breeze fronts and thunderstorm outflows) interacting with an existing temperature inversion. In this paper we describe a systematic laboratory study in a water channel, of internal bores and their generation by the movement of gravity currents through a two-layer model of the atmosphere. We compare the results of our laboratory experiments with previous theories and numerical simulations and with several detailed atmospheric observations of internal bores at different stages of development.

1. INTRODUCTION

A variety of atmospheric observations over the past 40 years have been interpreted as the result of internal bores or internal solitary disturbances propagating on low-level temperature inversions. Commonly the observations are described as an abrupt increase in ground-level pressure (several mb in a few minutes) followed by a sustained period of high pressure often consisting of wave-like oscillations. The increase in ground-level pressure is usually accompanied by an increase in ground-level temperature and a shift in the wind direction (so that the wind near the surface points in the direction of propagation of the disturbance). On occasion these disturbances have been observed to travel several hundred kilometres and their presence is sometimes associated with strong convective motions.

Some early observations were reported by Tepper (1950). He tracked the movement of squall lines across parts of the midwestern United States and deduced that they correlated with locally measured ground-level pressure jumps. He speculated that these pressure jump lines, as he called them, are evidence of a bore propagating along a nocturnal temperature inversion. He speculated further that the bore was produced by the impulsive motion of a cold front into the existing nocturnal inversion. Similar observations have been made in North America by, among others, Shreffler and Binkowsky (1981). They suggested that the interaction of cold thunderstorm outflows with an established temperature inversion may be the source of pressure jump lines. If this assumption is true, their data indicate that the pressure jumps had travelled over 500 km from their place of origin.

One of the best documented and most spectacular examples of atmospheric bores is the so-called Morning Glory which occurs near the southern coast of the Gulf of Carpentaria in northern Australia. It is described as a type of wind squall that is accompanied by a sharp rise in surface pressure, a change in wind direction and often is visible as a propagating roll cloud or sometimes a series of such clouds. Clarke *et al.* (1981) present convincing evidence that the Morning Glory is an undular bore propagating along a temperature inversion. In addition, they hypothesize that the Morning Glory is produced by the interaction of a sea-breeze front or katabatic winds with a nocturnal or

* Present address: Universities Space Research Association, NASA/Goddard Space Flight Center, Greenbelt, MD 20771, U.S.A.

maritime inversion. More recently, Smith *et al.* (1982) have proposed that some of the Morning Glories, in particular those that move in a northerly direction, are produced by a mesoscale front interacting with an existing temperature inversion.

The evidence is increasing that the Morning Glory is a not unusual type of atmospheric bore. Observations of Morning-Glory-like clouds have been made in southern Australia by Robin (1978), in Oklahoma, U.S.A. by Haase and Smith (1984) and in north-west Australia by Smith (1986). Smith *et al.* (1982) catalogue a variety of observations from around the world of atmospheric disturbances with pressure signatures similar to the Morning Glory, some with and some without the accompanying clouds.

The common feature of the proposed generation mechanisms for these bores is that they are the result of some type of gravity current moving into an existing temperature inversion. The distinguishing characteristic of a gravity current is that fluid of one density flows mainly horizontally into fluid of another density under the influence of gravity. Mesofronts such as sea-breeze fronts and thunderstorm outflows are typical atmospheric examples of gravity currents. Many more examples of atmospheric gravity currents are described by Simpson (1982, 1987).

Although there has been much speculation about gravity currents as a possible generation mechanism for atmospheric bores, hardly any direct evidence has been produced. That a gravity current moving into a stratified fluid can produce undular bores has been demonstrated in the laboratory experiments of Maxworthy (1980), Simpson (1982), Smith *et al.* (1982) and in the numerical simulations by Crook and Miller (1985). However, all these investigations have been in the way of feasibility studies, showing that it is possible for gravity currents to generate bores but not showing the full range of behaviour of bores and gravity currents in stratified fluids. Moreover, no quantitative comparisons have been made between these idealized results and direct observations in the atmosphere of a gravity current generating a bore. The attempts to do this so far, such as Crook (1983), have required guessing at the structure of the gravity current. In fact, to our knowledge no one has presented direct observations that have been interpreted as an atmospheric gravity current generating a bore.

The main purpose of the present paper is to provide some quantitative evidence in favour of the theory that atmospheric bores can be generated by the motion of a gravity current into an existing temperature inversion. We do this in two steps. First we describe some laboratory experiments in which we simulate in a water channel the motion of a gravity current into an idealized two-layer atmosphere. We make quantitative measurements of both the bore (which propagates along the interface between the two layers) and the gravity current driving the early stages of the developing motion over the full range of governing parameters relevant to atmospheric flows. And second, we compare our laboratory measurements quantitatively with a few detailed descriptions of bores in the atmosphere. In some cases, we were able to find evidence of developing bores and the gravity currents driving them by carefully scrutinizing existing observations. In these cases the evidence of the developing bores went unnoticed by the original authors of the papers describing these observations.

The organization of the paper is as follows. In section 2 we outline some results of non-mixing hydraulic theory for the flows produced by the motions of obstacles in two-layer fluids. We use these results as a framework for discussing, in section 3, our laboratory experiments. There were two sets of experiments. The first set is essentially an extension of the experiments performed by Wood and Simpson (1984), in which a bore is generated on the interface between two fluids of different density by towing a thin rounded obstacle along the bottom of a water channel. This series of experiments provides us with quantitative information about the structure of bores in two-layer

systems. In the second set we generate bores by introducing gravity currents, produced by fixed volume releases of salt water, into the two-layer channel. This set of experiments allows us to catalogue how the characteristics of the gravity currents determine the type of bores they generate on the fluid interface. In section 4, we compare our laboratory results with some previous theoretical and numerical work on the generation of bores by gravity currents in two-layer channels. We then, in section 5, compare our laboratory results with several well-documented atmospheric observations of internal bores in different stages of development. A summary of our results and some conclusions are given in section 6.

2. HYDRAULIC THEORY FOR TWO-LAYER FLOW OVER OBSTACLES

As a framework for discussing our experiments, we review here some results from the inviscid hydraulic theory for the flow of two non-mixing layers of fluid over a streamlined solid body. A sketch of the flow under consideration is shown in Fig. 1. A symmetric obstacle, with maximum height d_o is towed at speed U through a two-layer fluid of total depth H consisting of a thin layer of depth h_o and density ρ_1 beneath a much deeper layer of density ρ_2 ($\rho_1 > \rho_2$). We assume that h_o/H is small enough so that setting it equal to zero is a valid approximation in the theoretical treatment.

With the above assumptions, the flow in Fig. 1 is accurately described by the shallow-water equations for the lower layer with the acceleration due to gravity g replaced by the reduced gravity $g' = g(\rho_1 - \rho_2)/\rho_1$. In a reference frame in which the obstacle is at rest, we seek steady solutions of the shallow-water equations in a neighbourhood about the obstacle. As shown by Long (1954, 1970, 1972) and Houghton and Kasahara (1968), the possible time-independent solutions of the shallow-water equations for this flow configuration are determined by two nondimensional parameters: $F_o = U/(g'h_o)^{1/2}$ and $D_o = d_o/h_o$. Figure 2, adapted from Baines and Davies (1980), depicts the different types of possible flows and the regions in the (D_o, F_o) parameter space in which these solutions exist.

As depicted in Fig. 2, four categories of flows are possible: supercritical, partially blocked, completely blocked, and subcritical. The supercritical and subcritical flows are symmetric about the obstacle crest; in supercritical flow, which exists above the curve AE, the interface bulges over the obstacle, and in subcritical flow, which exists below the curve AB, the interface dips over the obstacle. The other types of flows are asymmetric about the crest of the obstacle. When the flow is partially blocked, which occurs when the parameters are in the region bounded by the curve CBAD, the flow changes from subcritical to supercritical at the crest and is connected to the far upstream and down-

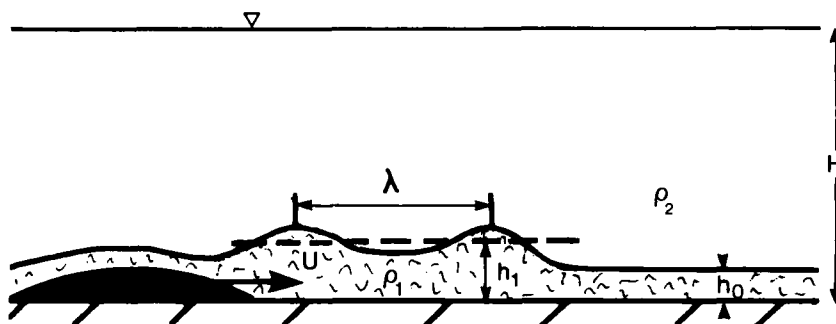


Figure 1. A sketch of two-layer flow over a streamlined obstacle.

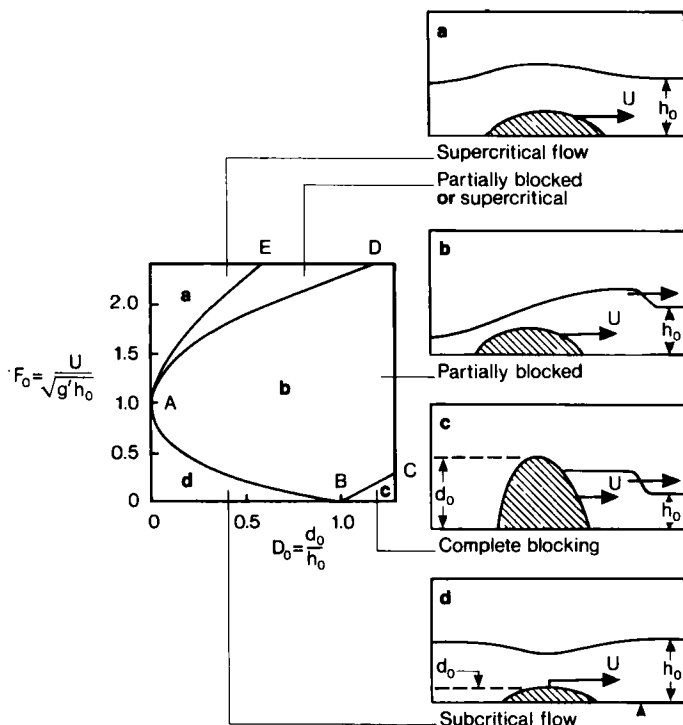


Figure 2. The flow regimes for two-layer flow over a streamlined obstacle (with the upper layer of infinite depth), adapted from Baines and Davies (1980).

stream levels of the lower layer by hydraulic jumps (bores) and long waves of expansion. In the mathematics of hydraulic theory, bores are propagating discontinuities in the interface level and fluid speed. For the case of completely blocked flow, which occurs below the curve BC, the lower-layer fluid is pushed in front of the obstacle in the form of a hydraulic jump and none of the fluid upstream of the obstacle ever passes over it. In the region between the curves AE and AD there are two possible solutions: supercritical flow or partially blocked flow; which of these two is obtained in any particular experiment depends on how the flow is initiated. The existence of both flow types in this region of the parameter space has been verified numerically by Pratt (1983). A more detailed description of all these types of flows is given by Houghton and Kasahara (1968) and more recently by Baines (1984).

In Fig. 2, the boundary curve AB+AD, which represents the largest value of D_o for which the steady solutions of the shallow-water equations are symmetric about the obstacle crest for a specified value of F_o , is given by

$$D_o = 1 - \frac{3}{2}F_o^{2/3} + \frac{1}{2}F_o^2. \quad (2.1)$$

The curve AE, which represents the values of D_o and F_o for which the speed of the upstream propagating bore has the same speed as the obstacle, is given by

$$D_o = -\frac{1}{4} - \frac{3}{2}F_o^{2/3} + \{1 + (1 + 8F_o^2)^{3/2}\}/16F_o^2 \quad (2.2)$$

and the curve BC, which represents the values of D_o and F_o for which the fluid speed in the lower layer upstream of the obstacle equals the obstacle speed, is given by

$$F_o = (D_o - 1)\{ \frac{1}{2}(1 + D_o)/D_o \}^{1/2}. \quad (2.3)$$

Implicit in the determination of the boundary curves AE and BC is a theory for the steady bore speed as a function of the bore strength (the ratio of the lower layer depths downstream and upstream of the bore) that gives

$$C/(g'h_o)^{1/2} = \{\frac{1}{2}(h_1/h_o)(1 + h_1/h_o)\}^{1/2} \quad (2.4)$$

where C is the bore speed in a reference frame in which the fluid upstream of the bore is at rest and h_1 is the mean depth of the two-fluid interface downstream of the bore. This theory, which is based on the principles of conservation of mass and momentum, assumes that fluid mixing and interfacial stress between the two layers are negligible.

When an upstream propagating bore exists, the bore strength h_1/h_o as a function of D_o and F_o is given by the transcendental equation

$$h_1/h_o = D_o - \frac{1}{2}u_1^2/(g'h_o) + \frac{3}{2}\{(h_1/h_o)u_1/(g'h_o)^{1/2}\}^{2/3} \quad (2.5)$$

where

$$u_1/(g'h_o)^{1/2} = F_o - (1 - h_o/h_1)C/(g'h_o)^{1/2} \quad (2.6)$$

in which u_1 is the speed (relative to the obstacle) of the fluid downstream of the bore.

The theoretical boundaries, represented by (2.1)–(2.3), between the different steady flow regimes have been verified partially by the numerical experiments of Houghton and Kasahara (1968) and the laboratory experiments of Long (1970). Our primary interest is in flows with upstream propagating bores (in particular, the partially blocked flows), so we designed our experiments so that the parameters D_o and F_o fell mostly within the curve CBAD.

3. LABORATORY EXPERIMENTS

Our experiments were performed in a perspex channel of rectangular cross-section, 348 cm long, 20.5 cm wide and usually filled to a depth of 50 cm. We modelled a low-level stable inversion as a thin layer of salt water beneath a much deeper layer of fresh water. The density of the salt water was generally between 0.5% and 2.0% greater than fresh water. The ratio of the depth of the salt water to the total depth of the fluid in the tank was fixed at 0.035.

(a) *The structure of internal bores in a two-layer system*

We used the technique described by Wood and Simpson (1984) to produce a bore propagating into two stationary layers. A streamlined obstacle that spanned the width of the channel was towed at a constant speed along the bottom of the tank. The obstacle had a semi-elliptical cross-section with a height of 5 cm and a length of 25 cm. The obstacle was accelerated rapidly from rest reaching its constant towing speed in just a few seconds after the motion was initiated. The resulting motion was photographed using the shadowgraph technique. The speed of the bore was measured by recording the times at which it crossed equally spaced marks on the perspex wall of the tank.

Our purpose here is to investigate how well the hydraulic theory outlined in the previous section describes bores in miscible fluids. In hydraulic theory, internal bores are idealized as travelling abrupt jumps in the level of the interface. In practice, internal bores are rarely observed as abrupt jumps. As described by Wood and Simpson, the character of the bore depends on the ratio h_1/h_o . The three types of bores we produced, which we have denoted as types A, B and C, are shown in the shadowgraph photographs in Fig. 3. A type A bore is observed when $1 < h_1/h_o < 2$. This bore has the smooth undular form shown in Fig. 3(a). The undulations are produced over the obstacle one

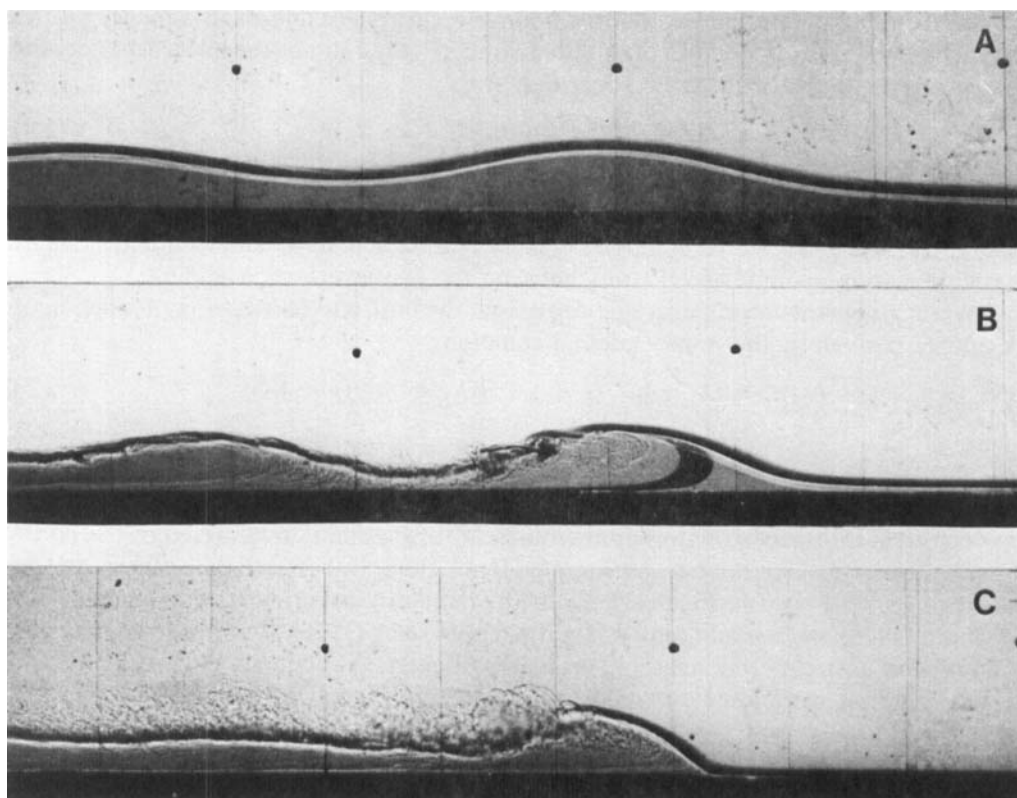


Figure 3. Photographs of the three types of bores generated by towing an obstacle through a two-layer fluid (as shown in Fig. 1): (A) a type A bore, smooth and undular; (B) a type B bore, some mixing downstream of the first crest; (C) a type C bore, has the appearance of a gravity current.

after another and travel upstream at a constant speed. Very little or no mixing between the two fluids is observed for bores of these strengths. A type B bore is observed when $2 < h_1/h_0 < 4$. This bore has the form shown in Fig. 3(b). In this case the bore is undular but some mixing, due to shear instability, occurs on the downstream face of the leading undulation. As h_1/h_0 gets close to 4 this mixing becomes more significant and occurs on the downstream faces of the first few undulations. A type C bore is observed when $h_1/h_0 > 4$. In this case the mixing completely dominates the motion, obliterating any undulations, as shown in Fig. 3(c). The bore then appears like a gravity current; this is clearly seen by comparing Fig. 3(c) with Fig. 1 in Britter and Simpson (1978).

It is interesting to compare these results with those for free-surface bores. As reported, for example, by Binnie and Orkney (1955), free-surface bores are smooth and undular when $1 < h_1/h_0 < 1.35$, have some wave breaking but are still undular when $1.35 < h_1/h_0 < 1.75$ and are fully turbulent when $h_1/h_0 > 1.75$. So, laminar internal bores can have much larger amplitude undulations than free-surface bores. A big distinction between free-surface and internal bores arises in the mixing process. The air entrained by turbulent free-surface bores is eventually detrained farther downstream, whereas the mixed fluid in an internal bore remains as a mixed layer left behind as the bore propagates forward. This means that conditions far downstream of the free-surface bores are unaffected by the air entrainment, but internal bores are significantly affected by the mixing.

Of course, when mixing occurs in internal bores the definition of the quantity h_1 becomes problematical because a sharp interface no longer exists. For experimental

convenience, we defined h_1 in these cases as the top of the mixed layer. Using this definition for h_1 , we have plotted our experimental measurements of the bore speed as a function of the bore strength in Fig. 4 along with the curve representing (2.4), the classical two-layer theory for the bore speed for non-mixing bores. The agreement is very good when there is no mixing, $1 < h_1/h_0 < 2$, but when there is mixing, $h_1/h_0 > 2$, the theory overpredicts the speed. This is because with the definition we have used for h_1 the two-layer theory overestimates the hydrostatic pressure increase across the bore when there is mixing. To correct the theory for the speed requires a method for predicting the vertical distribution of density downstream of the bore when mixing occurs. We are not aware of any simple means for doing this.

However, as discovered by Wood and Simpson (1984), when $h_1/h_0 > 2$ (with h_1 defined as the top of the mixed layer) the bore speed is quite well described as the speed of a gravity current with head height h_1 . For gravity currents with $h_1/H < 0.075$, Huppert and Simpson (1980) provide the following empirical formula for the front speed†

$$C/(g'h_1)^{1/2} = 1.19 \quad (3.1)$$

which can be adapted to our present needs as

$$C/(g'h_0)^{1/2} = 1.19(h_1/h_0)^{1/2}. \quad (3.2)$$

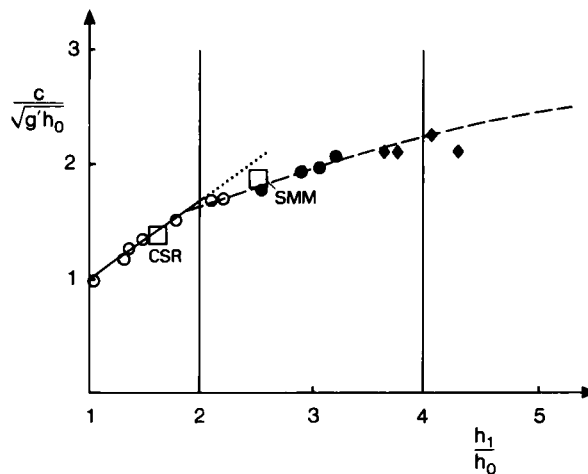


Figure 4. The bore speed as a function of the bore strength. The solid line is (2.4), the dashed line is (3.2). The symbols \circ , \bullet , and \blacklozenge represent our laboratory measurements (\circ represents a type A bore, \bullet a type B bore and \blacklozenge a type C bore). The \square are atmospheric measurements as described in section 5: CSR, Clarke *et al.* (1981); SMM, Simpson *et al.* (1977).

This curve is plotted in Fig. 4 as a dashed line and shows close agreement with the experimental results. So bores in two-layer fluids *appear* like gravity currents when $h_1/h_0 > 4$, but they *behave* like gravity currents when $h_1/h_0 > 2$.

For the cases when the bore is undular ($1 < h_1/h_0 < 4$), we have attempted to measure the wavelength and amplitude of the undulations. These are plotted in Figs. 5 and 6 as functions of h_1/h_0 . Also included in these plots are data points from some atmospheric observations that are discussed later in the present paper. There is a significant amount of scatter in these results, but based on the theory of Benjamin and

† The reader may realize that when $h_1/h_0 > 2.14$ then $h_1/H > 0.075$ since $h_0/H = 0.035$ in our experiments. However, the correction to (3.2), which reduces the speed, is less than 15% when $2.14 < h_1/h_0 < 4$.

Lighthill (1954) this is to be expected. They showed that undular free-surface bores can exist only if some energy is dissipated by frictional forces. Furthermore, the amplitude and wavelength of the undulations are rather sensitive functions of how much energy is lost owing to friction. Therefore, the measurements we show in these two plots are sensitive to small variations in the experimental conditions.

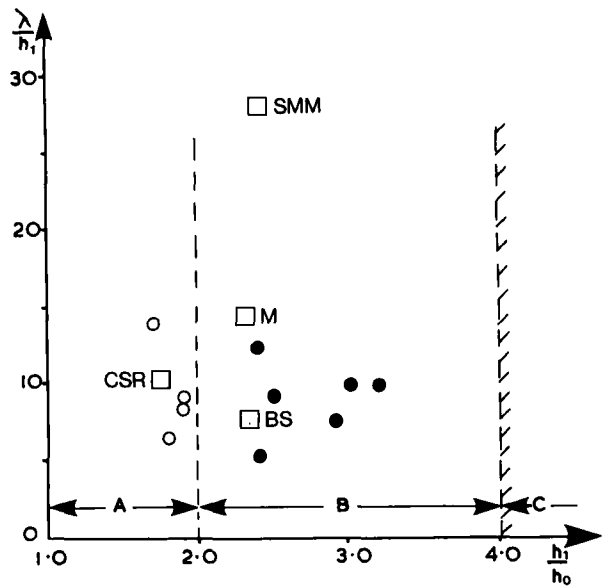


Figure 5. The measured wavelengths of types A and B bores as functions of the bore strength. The symbols ○ and ● represent our laboratory measurements (○ represents a type A bore and ● a type B bore). The □ are atmospheric measurements as described in section 5: BS, Bedard and Sanders (1978); CSR, Clarke *et al.* (1981); M, Marks (1974); SMM, Simpson *et al.* (1977).

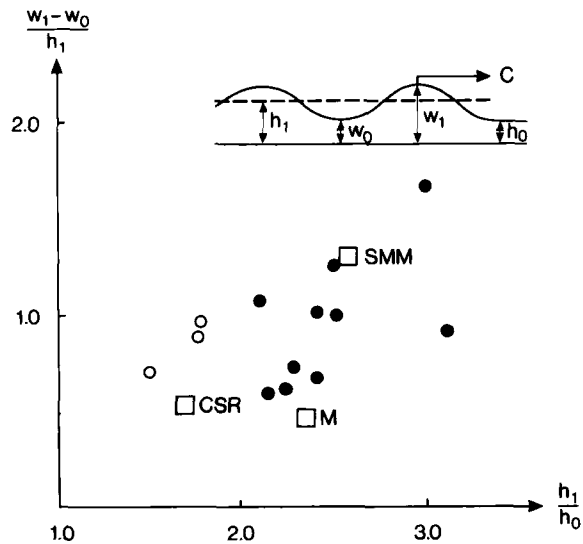


Figure 6. The measured values of the amplitude of the undulations for types A and B bores. The symbols ○ and ● represent our laboratory measurements (○ represents a type A bore and ● a type B bore). The □ are atmospheric measurements as described in section 5: CSR, Clarke *et al.* (1981); M, Marks (1974); SMM, Simpson *et al.* (1977).

Baines (1984, 1987) has presented some results from experiments similar to ours except that he worked with immiscible fluids. His results agree with ours for the speed of the upstream propagating bore, up to the point where the bore begins to show signs of turbulent mixing. Baines did not generate bores with strengths much larger than this.

(b) *Generation of internal bores by gravity currents*

The technique we used to produce gravity currents is illustrated in Fig. 7. The technique is similar to that described in Rottman and Simpson (1983). After the tank had been filled with the two layers of fluid, a water-tight barrier (called a *lock gate*) was inserted into the tank at some fixed distance from one of the end walls to create a *lock*. Once the gate was securely in position, salt water (usually only slightly heavier than the fluid in the lower layer) was pumped slowly through the floor into the lock until the heavy fluid reached a prescribed depth D . The experiment was begun by rapidly removing the gate completely from the tank by hand. Similar methods to those described previously were used to record and measure the motion. In addition a video recording was made of each experiment.

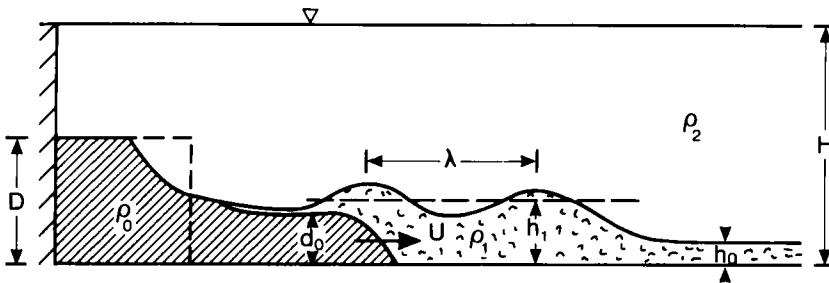


Figure 7. A sketch of our laboratory experiments on a gravity current produced by a lock release into a two-layer fluid.

A fixed volume release was used in our experiments instead of a constant input of dense fluid on the grounds of simplicity. It has been shown by Rottman and Simpson, in their experiments on fixed volume releases into a neutrally stratified surrounding fluid, that in the initial stages the current from such a release flows at a constant speed and depth away from the lock. This regime extends from three to ten times the original lock length, depending on the fractional depth of the dense fluid. In the present experiments, three times the lock length is greater than the total length of the tank, so a constant velocity and depth are expected for the gravity current until it reaches the end of the tank.

By adjusting the depth D and the relative densities of the three fluids, we were able to produce gravity currents that generated all three types of bore described in the previous section. When the gate was removed the heavy fluid began to move forward as a gravity current. A fairly reliable rule seemed to be that the depth of the gravity current would be about $D/2$. Usually the first sign of the generation of a bore on the lower layer was a change in the nature of the gravity current head. A bore of type A begins as a smooth hump that encloses the gravity current head and then moves forward along the interface between the two layers. As it moves forward the bulge tends to take with it a small amount of the gravity current fluid and the gravity current front is disrupted. The small amount of fluid taken from the gravity current front is soon left behind as the bore

advances. Figure 8 shows a sequence of photographs of a gravity current producing a type A bore. The description is similar for type B bores except more gravity current fluid is carried forward by the waves than in type A.

The bores of type C, as described in the previous section, appear very similar to gravity currents. We found that whenever a type C bore was generated its speed was not measurably different from the speed of the gravity current driving it. That is, the bore was stationary relative to the gravity current front and remained some fixed distance in front of the current. In some cases the bores were formed so close to the gravity current front that the two became indistinguishable, except that the gravity current became somewhat altered in structure and velocity. Technically, since the obstacle speed and bore speed are the same, these types of flows are on the border line between the partially blocked and supercritical categories. In the cases in which a type C bore was distinguishable from the gravity current front the periodic shedding of the gravity current front that occurs with the types A and B bores does not occur.

Because the types A and B bores periodically carried away portions of the front of the gravity current nose, it was somewhat difficult to define a gravity current speed. In these cases we defined an average speed of the gravity current in terms of the distance

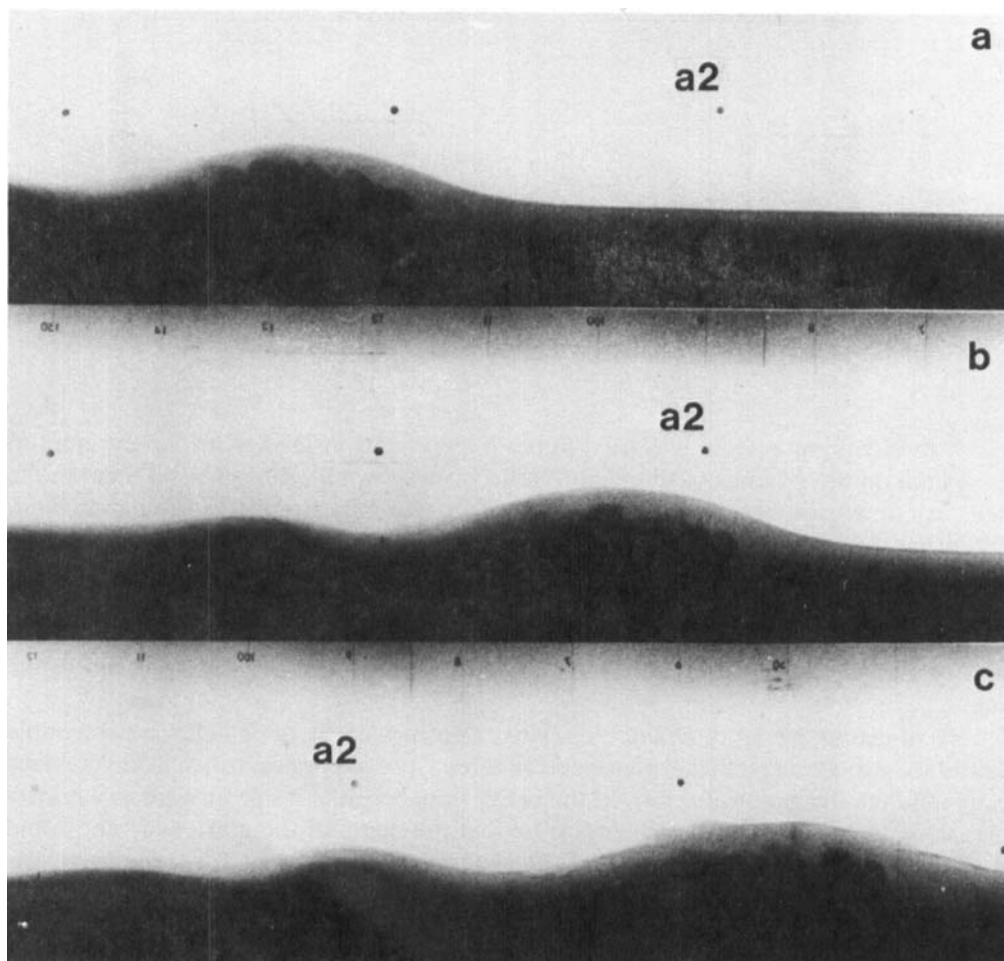


Figure 8. Sequential photographs of the early stages of the generation of a type A undular bore by a gravity current in our experiments.

travelled at the time when each new front was formed. We found that the procedure gave a fairly constant rate of advance of the current which was about 0.75 times the bore speed for type A bores, increased through 0.9 for type B bores and reached 1.0 for type C bores.

Dimensional analysis shows that, with the Boussinesq approximation, the speed of the gravity current in this two-layer configuration with the upper layer much deeper than the lower layer is given by

$$U/(g'h_0)^{1/2} = f(D_0, \alpha) \quad (3.3)$$

where

$$\alpha = (\rho_0 - \rho_1)/(\rho_1 - \rho_2) \quad (3.4)$$

in which ρ_0 is the density of the gravity current and as before $D_0 = d_0/h_0$ except that now d_0 is the height of the gravity current head (instead of the obstacle height). In Fig. 9 we have plotted $U/(g'h_0)^{1/2}$ as a function of D_0 for various values of α . This is similar to the plot in Fig. 2 if we equate the height of the obstacle to the height of the gravity current head. In essence we are seeing how much the gravity current acts like a solid obstacle. Also plotted on this graph are the boundary curves (described in section 2) separating subcritical and supercritical flow from partially and completely blocked flow. The types of bore (A, B or C) produced by each gravity current, or the type of flow (subcritical or supercritical) if no bore was produced, are distinguished by the form of the points, and adjacent to each point of the graph is a number indicating the value of α .

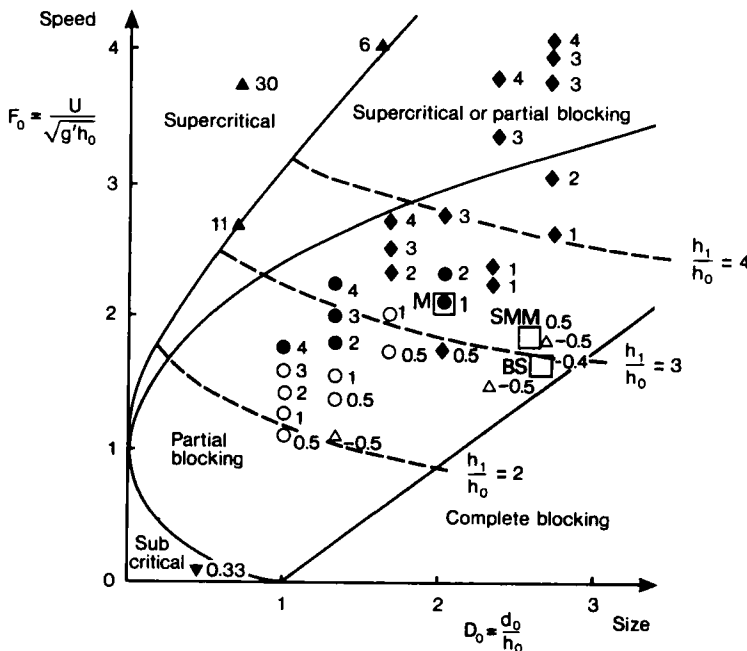


Figure 9. A plot of our experimental results in the (D_0, F_0) parameter space. The solid lines are the boundary curves plotted in Fig. 2. The points are our experimental values. The symbols used to plot each point denote the type of flow observed: ▼, subcritical gravity current; ▲, supercritical gravity current; ○, type A bore; ●, type B bore; ◆, type C bore; △, an intrusion. The □ are atmospheric measurements as described in section 5: BS, Bedard and Saunders (1978); M, Marks (1974); SMM, Simpson *et al.* (1977). The number next to each point is the value of α .

In general the points fit into the hydraulic theory of flow over an obstacle fairly well. We found subcritical and supercritical flows over the gravity current in the parameter regimes where we expected to see them. Photographs of these two types of flows are shown in Fig. 10. The flows with upstream propagating bores occurred only in the region of the parameter space between the boundary curves for the theoretical existence of such flows.

It is encouraging that the general features of the gravity current flows fit in with the theory for flows over solid obstacles, even though the boundary curves AE and BC are dependent on (2.4) which was found to be inaccurate for bores with $h_1/h_0 > 2$. A more

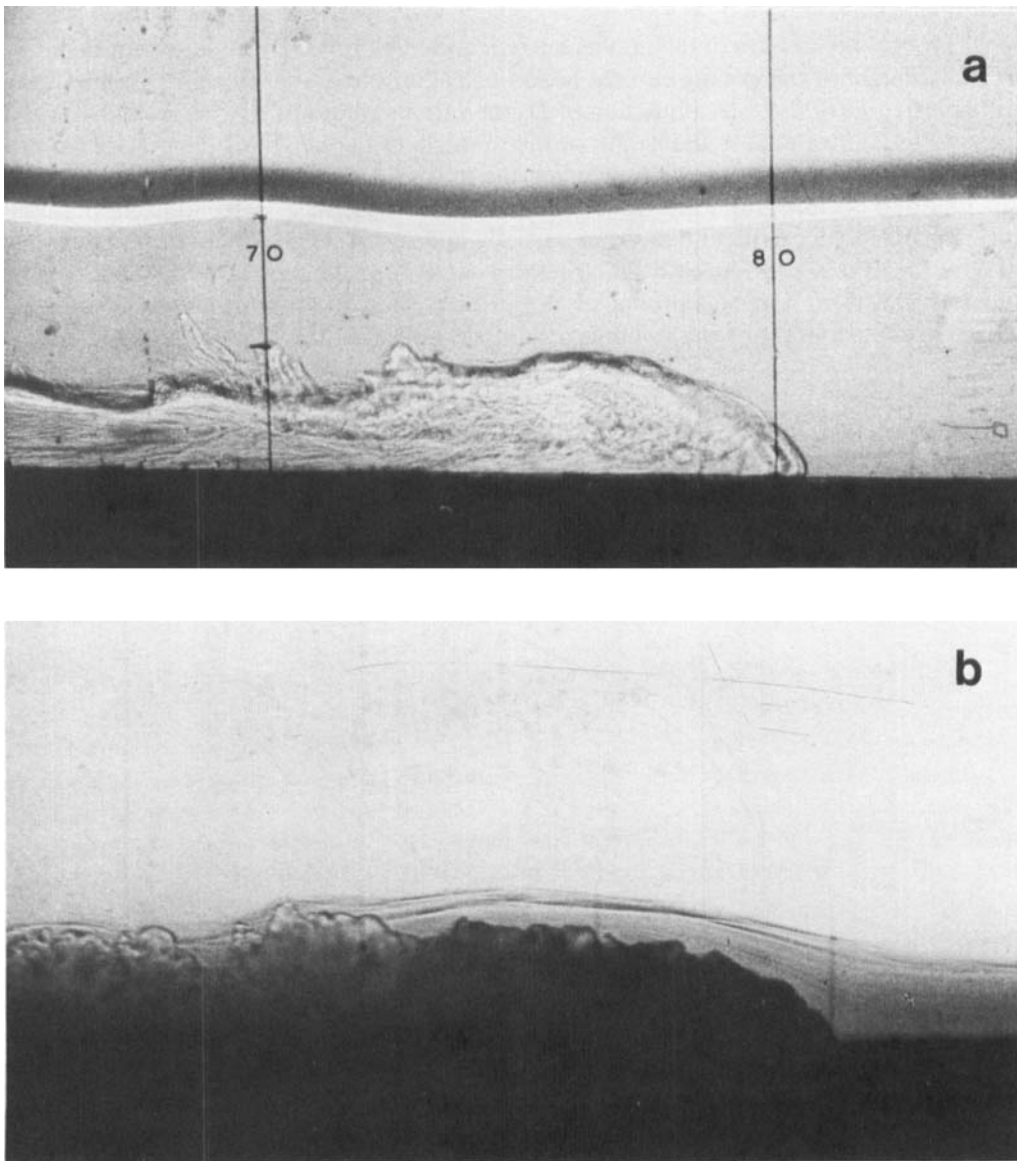


Figure 10. Photographs of gravity currents that did not produce internal bores: (a) a subcritical gravity current; and (b) a supercritical gravity current.

detailed look at the data shows, however, that the theory is only a rough approximation to our laboratory results. Table 1 lists the measured quantities for each experiment in which a type A or B bore was observed and in parentheses we have shown the values for the strength and speed of the bore predicted by the hydraulic theory of section 2 corresponding to the observed values of the gravity current speed and height. The theory seems to have the same trends as the data but quantitatively is in error by as much as 40%. Unexpectedly, the theory seems to be best at predicting the bore strength when the bore generated by the gravity current is of type B.

TABLE 1. A LIST OF THE EXPERIMENTAL RESULTS FOR THE TYPES A AND B BORES CORRESPONDING TO THE DATA POINTS PLOTTED IN FIG. 9 AND COMPARISON WITH TWO THEORIES

Exp.	d_o/h_o	$U/(g'h_o)^{1/2}$	α	h_i/h_o	$C/(g'h_o)^{1/2}$	Type
RS1	1.0 [0.6]	1.1	0.50	1.6 (2.0) [1.8]	1.4 (1.7) [1.6]	A
RS2	1.3 [0.7]	1.4	0.50	1.7 (2.4) [2.1]	1.6 (2.0) [1.8]	A
RS3	1.7 [0.8]	1.5	0.50	2.0 (2.6) [2.2]	1.8 (2.2) [1.9]	A
RS4	1.0 [0.5]	1.2	1.00	1.7 (2.0) [1.8]	1.5 (1.8) [1.6]	A
RS5	1.3 [0.5]	1.5	1.00	2.0 (2.5) [2.1]	1.7 (2.1) [1.8]	A
RS6	1.7 [0.6]	1.8	1.00	2.8 (2.9) [2.4]	2.0 (2.4) [2.0]	A
RS7	1.0 [0.3]	1.2	2.00	2.0 (2.0) [1.6]	1.6 (1.7) [1.4]	A
RS8	1.0 [0.3]	1.6	3.00	2.1 (2.4) [1.9]	1.7 (2.0) [1.7]	A
RS9	2.0 [0.7]	2.1	1.00	3.4 (3.3) [2.8]	2.2 (2.7) [2.3]	B
RS10	1.3 [0.4]	1.7	2.00	2.8 (2.7) [2.2]	2.0 (2.2) [1.9]	B
RS11	1.3 [0.3]	1.9	3.00	2.9 (2.8) [2.3]	2.0 (2.3) [1.9]	B
RS12	1.0 [0.2]	1.6	4.00	2.3 (2.4) [1.9]	1.8 (2.0) [1.7]	B
RS13	1.3 [0.3]	2.1	4.00	3.2 (3.1) [2.4]	2.3 (2.5) [2.0]	B

The values in parentheses were obtained from the theory outlined in section 2 for specified values of d_o/h_o and $U/(g'h_o)^{1/2}$, and the values in square brackets were obtained from the theory in section 4 for specified α and $U/(g'h_o)^{1/2}$.

The only type of flow that we could not generate with a gravity current was a completely blocked flow. In the experiments with gravity currents, in contrast to those with a solid obstacle, the two parameters D_o and F_o are related to each other as indicated by (3.3), and experiments show that F_o is an increasing function of D_o . But just the opposite behaviour is required to produce a completely blocked flow: the obstacle must be relatively high and move relatively slowly. As shown in Fig. 9, as the experimental parameter values approach the boundary curve for blocked flow, the parameter α approaches zero. That is, when we attempted to generate a gravity current that would completely block the lower layer we generally ended up with an *intrusion*; that is, a gravity current that travels along the interface with a density between the densities of the two fluids in the layers (i.e. with $\alpha < 0$). Figure 11 shows a photograph of such an intrusion and the undular bore it has generated. Our observations show that the phenomenon of intermittent fronts does not occur in bores generated by intrusions.

4. COMPARISON WITH THEORETICAL AND NUMERICAL MODELS FOR GRAVITY CURRENTS IN TWO-LAYER FLUIDS

It is of some interest to compare the results of our experiments with Crook's (1983) analytical theory for energy-conserving gravity currents in a two-layer fluid. Although the gravity currents in our experiments do not appear to be energy-conserving, evidence does exist that this energy-conserving theory might be a useful approximation. For example, Crook and Miller (1985) found that this theory compared well with the results of their numerical simulations of gravity currents in two-layer fluids, which included a first-order turbulence closure model.

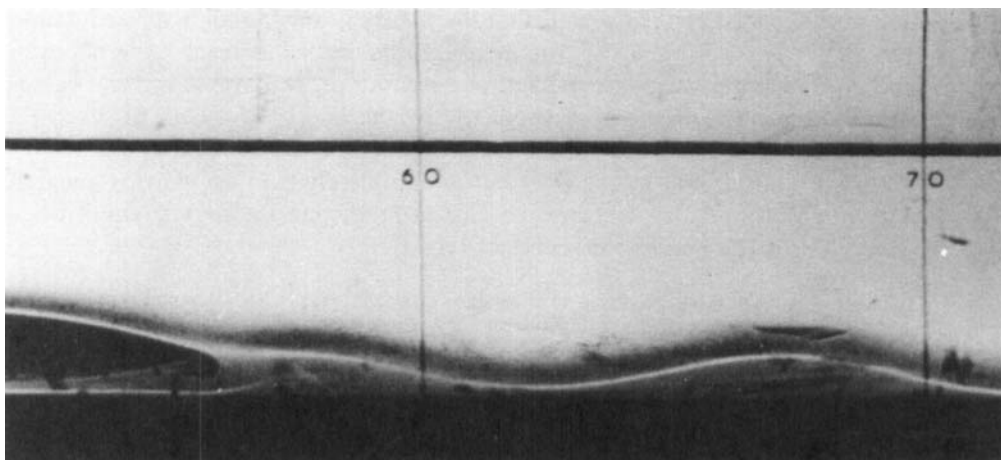


Figure 11. A photograph of an intrusion generating an undular bore on the interface between two fluids of different densities in the laboratory.

The theory Crook (1983) developed is basically an extension of the steady, energy-conserving theory of Holyer and Huppert (1980) for gravity currents in two-layer fluids (for the limiting case when the upper layer has infinite depth) to allow for the presence of an upstream hydraulic jump, as illustrated in Fig. 12. Holyer and Huppert assume that the flow in and around the gravity current is steady and irrotational and that the density in each layer and in the gravity current is uniform (implying that there is no mixing between the fluids of different densities). They apply the integral forms of the principles of mass and momentum conservation and use Bernoulli's equation along streamlines (implying energy conservation) to obtain the following relations:

$$1 - 2(d_1/h_1) + \alpha\{1 - (d_1/h_1)^2\}\{1 - (d_1/h_1)\}^2 = 0 \quad (4.1)$$

$$d_o/h_1 = (1 - d_1/h_1)/[1 + \alpha\{1 + (d_1/h_1)^2\}] \quad (4.2)$$

$$c_1/(g'h_1)^{1/2} = (2\alpha d_o/h_1)^{1/2}(d_1/h_1) \quad (4.3)$$

where d_1 is the depth of the lower layer of fluid over the gravity current and c_1 is the fluid speed (relative to the gravity current) in the lower layer upstream of the gravity current. For a specified value of α , (4.1) can be solved numerically for d_1/h_1 and then (4.2) and (4.3) give d_o/h_1 and $c_1/(g'h_1)^{1/2}$ explicitly; that is, for specified α the gravity current is completely specified in terms of the upstream depth h_1 .

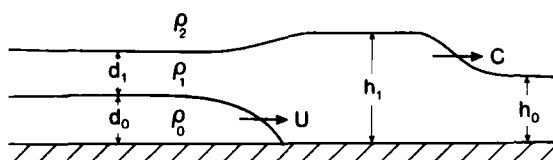


Figure 12. A sketch of an idealization of a gravity current driving a bore in a two-layer fluid in which the depth of the upper fluid layer is infinite. U is the gravity current speed and C the bore speed in the laboratory reference frame, in which the fluid upstream of the bore is at rest.

Applying the principles of conservation of mass and momentum similarly to the upstream propagating bore, Crook (1983) obtained the additional relation:

$$U/(g'h_o)^{1/2} = c_1/\{(g'h_1)^{1/2}(h_1/h_o)^{1/2}\} + C/(g'h_o)^{1/2}(1 - h_o/h_1) \quad (4.4)$$

where C and U are the speeds of the bore and the gravity current, respectively, in the laboratory reference frame (in which the fluid upstream of the bore is at rest) and C is given in terms of h_1/h_o by (2.4). So, for a specified value of h_1/h_o , (4.4) is an explicit expression for the gravity current speed given the results of (4.1)–(4.3) for any required value of α . Alternatively, we could specify $U/(g'h_o)^{1/2}$ and solve (4.4) for h_1/h_o for a given α .

The results of this theory for $U/(g'h_o)^{1/2}$ as a function of d_o/h_o for specified α are plotted in Fig. 13. Similar to Fig. 9, this plot shows also the region of the parameter space in which energy-conserving gravity currents can exist. The upper boundary curve is where the gravity current speed equals the bore speed and is the same as AE in Fig. 2. The lower boundary curve is where $h_1/h_o = 1$, and the final boundary curve is where $\alpha = 0$. Outside of this region the gravity currents must be dissipative or an intrusion. Inside the region where energy-conserving gravity currents can exist we have plotted curves of constant α . Also plotted in this graph (as dashed lines) are the curves for the strengths of the bores associated with the gravity currents of a particular speed and height.

We mention that the $\alpha = 0$ curve intersects the D_o axis at $D_o = 0.5$ and not at $D_o = 1.0$ as one might expect. This is because as α approaches zero the density difference between the gravity current and the lowest layer becomes very small compared with the

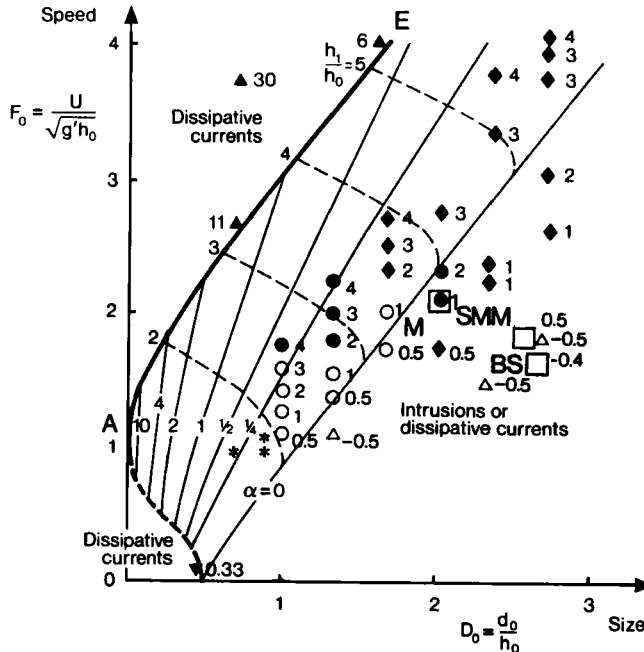


Figure 13. A plot of the (D_o, F_o) parameter space for energy-conserving gravity currents as depicted in Fig. 12. Energy-conserving gravity currents can exist only in the region between the heavy solid curve marked AE (which is where $U = C$), the solid curve labelled $\alpha = 0$ and the dashed curve labelled $h_1/h_o = 1$. Outside of this region the gravity currents must be dissipative or intrusions. The solid lines indicate constant values of α and the dashed lines constant values of the bore strength h_1/h_o . The plotted points are as in Fig. 9, except the * represent the numerical simulations of Crook and Miller (1985) that are listed in Table 2.

density difference between the two layers of fluid. Thus the interface between the two layers is like a solid lid to the gravity current and energy-conserving gravity currents must occupy precisely half the depth in these cases, as shown by Benjamin (1968).

We have plotted in Fig. 13 our experimental results from Fig. 9. It appears from this plot that the experimental results do not compare well with the theory. However, a more complete comparison, shown in Table 1, reveals that, although the theory greatly underpredicts the observed gravity current height, it fairly accurately predicts (typically, within 10% for the type A bores and within 25% for type B bores) the bore strength and speed. It is the underprediction of gravity current height that makes the comparison in Fig. 9 look so bad. The gravity current height is the most difficult quantity to measure in our experiments, and additionally it is difficult to define a height for a mixing gravity current that is relevant to a non-mixing theory. We conclude that, despite the fact that our gravity currents are not energy-conserving, the theory does a good job (particularly for type A bores) of predicting those quantities that can be clearly defined and accurately measured in our experiments.

Crook (1983) noted some difficulties in comparing this energy-conserving theory with some field observations of the Morning Glory. However, there are many more reasons why an atmospheric comparison with the theory may be poor. For example, the stability and vertical velocity structure of the atmosphere may not be well modelled by the two-layer idealization assumed in the theory.

TABLE 2. A LIST OF THE RESULTS FROM THE NUMERICAL SIMULATIONS OF TYPE A BORES BY CROOK (1984) AND CROOK AND MILLER (1985) AND COMPARISON WITH THE ENERGY-CONSERVING THEORY

Exp.	d_o/h_o	$U/(g'h_o)^{1/2}$	α	h_1/h_o	$C/(g'h_o)^{1/2}$	Type
CM1	? [0.8]	1.0	0.26	1.9 [2.0]	1.3 [1.4]	A
CM2	? [0.9]	1.1	0.20	1.9 [2.2]	1.4 [1.4]	A
CM3	? [0.9]	1.0	0.14	1.9 [2.1]	1.3 [1.4]	A

Values in square brackets are from energy-conserving theory for gravity currents in two-layer fluids for specified values of α and $U/(g'h_o)^{1/2}$, as outlined in section 4.* Because of smoothing of the density profile in the simulations, the depth of the gravity current, d_o , is difficult to determine with any precision and therefore no value is listed.

* To obtain the results shown in the table, we followed Crook and Miller (1985) in modifying the theory of section 4 to include the $O(h_o/H)$ correction (with $h_o/H = 0.125$) in the formula for the bore speed but continued to use Holyer and Huppert's (1980) theory for the gravity current that assumes $h_o/H = 0$. Crook (private communication) claims that his numerical results show some justification for this apparent inconsistency.

The results of the three numerical simulations described in Crook and Miller (1985) are compared with the results of this simple energy-conserving theory in Table 2. The theory predicts the computed bore strength and speed to within 15%. Note that because of the necessary smoothing in the numerical simulations it is difficult to define precisely the depth of the gravity current. However, a rough 'eyeball' estimate of D_o from the potential temperature plots for these computer simulations (shown in Crook 1984) agrees with the theoretical values in the table. Using the theoretical values of D_o and the numerically obtained values of F_o , we have plotted the three cases Crook and Miller presented in our Fig. 13.

5. COMPARISON WITH ATMOSPHERIC OBSERVATIONS

There are many reported observations of atmospheric bores but details of the bores' early stages of development are hard to find. In this section we will examine one observation of an atmospheric bore for which the generating gravity current was not directly observed, two observations that appear to show directly the early stages of generation of an atmospheric bore by some type of gravity current, one observation of a supercritical gravity current and one observation of an intrusion that is possibly producing a bore. For convenience in comparing the atmospheric observations with our two-layer laboratory experiments, we will present in each case a plot of the flow in which the density structure has been simplified. In general this means that the potential density is averaged over layers in which it changes fairly slowly, so that the density field will be in layers of constant potential density. In all five cases described here, this procedure resulted in a two-layer density structure with the lower layer much shallower than the upper layer.

In general, the structure of the lower atmosphere is more complicated than our simple two-layer model. When most atmospheric bores are observed the atmosphere is more accurately described as two layers of uniform stability with the lower layer shallower and more strongly stable than the upper layer; for example, the Morning Glory usually propagates into two layers in which the ratio of the buoyancy frequency in the lower layer to that in the upper layer is about three or four.

It is prudent to consider the extent to which our simple two-layer model is applicable to bores in layered continuously stratified fluids. Although a direct analogy between the two is not possible, Durran (1985) has shown, in the context of severe downslope winds, that two-layer continuously stratified flow has strong qualitative similarities to simple two-layer flow near the obstacle driving the motion (the mountain in his case and the gravity current in ours) when the lower layer is more strongly stratified than the upper layer. Based on Durran's results, we expect our simple two-layer model to compare well qualitatively with atmospheric observations of the initial stages of bore formation by a gravity current—when the gravity current is not far from the leading edge of the bore.

Crook (1986, 1988) has shown that a bore propagating some distance in front of a gravity current will lose its energy very rapidly to vertically propagating gravity waves in the upper layer of a two-layer continuously stratified fluid. Crook suggests that for a bore to propagate any significant distance some mechanism must be in place to trap the vertically propagating waves. He proposes, based on numerical simulations, three possibilities: (1) upper-level opposing winds; (2) lower-level opposing winds; and (3) an inversion at some height in the upper layer; and shows that at least one, and sometimes all three of these mechanisms have been in place when an atmospheric bore has been observed to propagate a significant distance. We expect that there may be some trouble in comparing our simple two-layer model with atmospheric observations of mature bores; the properties of the atmospheric bores will depend on the efficiencies of the trapping mechanisms in place. The comparison is also complicated by the presence of moisture in the atmosphere. Crook (1986) shows that cloud formation as seen in the Morning Glory tends to reduce the amplitude and increase the wavelength of bore undulations.

(a) *Observations of a type A bore*

The Morning Glory that appeared over Burketown, Australia on the morning of 4 October 1979 was particularly well documented by Clarke *et al.* (1981) and Smith and Goodfield (1981). A light aeroplane, pilot balloons and several ground stations were used to measure the structure of the atmosphere and of the propagating undular bore. The bore was also recorded as it approached Burketown by time-lapse photography.

We have taken the measured profiles of virtual potential temperature and velocity and constructed the two-layer idealization of the flow as sketched in Fig. 14(a). The sketch reveals an undular bore with a strength h_1/h_0 of about 1.6 propagating along the density interface. This strength identifies the bore as in our type A category; that is, we expect this bore to have a smooth undular shape with no significant shear-generated turbulence on the downstream faces of the undulations. The relative streamlines (deduced from balloon trajectories) and measurements of the ground-level pressure and wind speed reported in Clarke *et al.* (1981) clearly show that the bore consisted of 4 or 5 undulations: in fact, five distinct cloud lines were observed. However, it is difficult to confirm the absence of turbulence in the atmospheric observations of the bore, although turbulence was reported to be 'notably slight' along the flight paths taken through the bore. The measured values of the speed of the bore, the wavelength of the initial undulation and the amplitude of this undulation are plotted in Figs. 4, 5 and 6, respectively, and compare well with our laboratory results.

The generation of this bore was not observed directly. In fact, based on the numerical simulations of Crook (1986), the presence of clouds at the crest of the undulations indicates that the gravity current driving this bore was probably decelerating and an appreciable distance behind the first undulation. So, based on our previous discussion we are somewhat surprised the observations compare so well with our experiments.

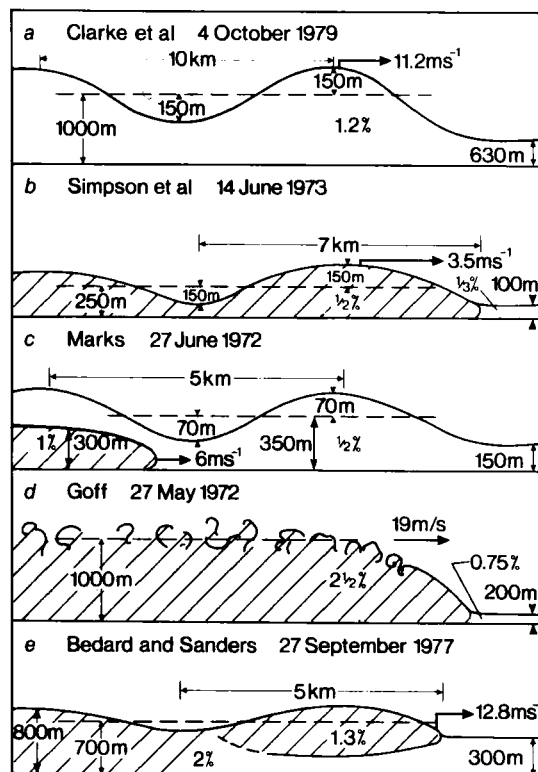


Figure 14. Two-layer idealizations of gravity currents and bores constructed from atmospheric observations: (a) a type A bore (the Morning Glory), from Clarke *et al.* (1981); (b) a type A bore generated by a sea-breeze front, from Simpson *et al.* (1977); (c) a type B bore generated by a thunderstorm outflow, from Marks (1974); (d) a supercritical gravity current (a thunderstorm outflow), from Goff (1976); and (e) a type B bore generated by a thunderstorm outflow of the intrusive type, from Bedard and Sanders (1978). The percentages shown in the figures are values of $(\rho_1 - \rho_2)/\rho_2$, where ρ_1 is the density of the layer in which the percentage appears.

(b) *Evidence of the generation of a type B bore by a sea-breeze front*

Simpson *et al.* (1977) report a study of the sea breeze in southern England in which a light aeroplane, pilot balloons and numerous ground stations were used to track the progress of the sea breeze as it moved inland. On 14 June 1973 they tracked a sea-breeze front as it intruded into a developing evening inversion.

Observations of the fields of potential temperature, humidity and wind were made during the hour before sunset. They showed that although the sea-breeze front in the early afternoon had been of the normal gravity current form, the foremost part of the sea breeze was then almost separated from the following flow. The length of this separated section of the sea breeze was measured to be about 7 km and was taken to be the wavelength of the disturbance. The mean height of the sea-breeze current at this point was measured to be about 250 m and the measured mean height of the developing inversion was about 100 m. Farther inland the arrival of the separated sea-breeze front was timed at four stations. The measured speed of the disturbance was about 3.5 m/s and the wavelength of the disturbance increased to 9 km. Other measurements of the wavelengths of disturbances of this type gave an average value of about 10 km.

Simpson *et al.* describe this separated part of the sea breeze, following Clarke (1965), as a sea-breeze *vortex*. In light of the present discussion, it is probably more accurate to describe this as an incipient internal bore propagating along the newly formed evening inversion and driven by the sea-breeze front. An idealized diagram of the flow, based on the measured potential temperature, is shown in Fig. 14(b). The strength of this bore is about 2.5, which according to our laboratory results makes it a type B bore. We expect a type B bore to have some shear-generated turbulence on the downstream faces of the undulations, but this cannot be confirmed from the atmospheric observations. Since the bore was caught in the very early stages of development, we cannot distinguish the bore speed from the sea-breeze front speed and we have plotted the speed of 3.5 m/s as the bore speed in Fig. 4 and gravity current speed (for which $\alpha = 0.52$) in Fig. 9, although we suspect that the true gravity current speed is somewhat less than this. The measured values of the wavelength and the wave amplitude of the bore are plotted in Figs. 5 and 6, respectively, as functions of the strength. All these comparisons with our laboratory results are reasonable except the comparison for the wavelength, for which the measured value is much larger than expected.

(c) *Evidence of the generation of a type B bore by a thunderstorm outflow*

Details of the early stages in the formation of a solitary disturbance on a low-level temperature inversion can be deduced from the pressure and temperature measurements of Marks (1974). The measurements were obtained from the 461 m meteorologically instrumented tower located about 6 miles north of Oklahoma City, U.S.A. The particular observations we are interested in occurred just after an isolated thunderstorm, travelling east, passed over Oklahoma City on 27 June 1972.

We constructed the idealized two-layer diagram of the flow shown in Fig. 14(c) based on the time history of temperature and pressure measurements made at the tower. The diagram shows that an initial pressure rise of about 1.1 mb in 9 min was due to the passage of a wave propagating on the existing 150 m temperature inversion. The diagram also shows that the wave is followed shortly by a gravity current of cold air (with a density ratio $\alpha = 1.0$) travelling at a speed of 6 m/s, probably produced by the thunderstorm to the south. The pressure decreased after the crest of the wave passed over the tower but later reached a new peak when the gravity current head reached the tower.

The diagram shows that the inversion height after the passage of the wave had an average value of about 350 m, so this disturbance was apparently a bore of strength 2.3. The strength identifies this bore as in our type B category. But, as in the previous case, we do not have sufficient observational data to confirm the existence of shear-generated turbulence on the downstream face of the first wave. However, the bore speed, wavelength and wave amplitude, plotted in Figs. 4, 5 and 6, respectively, compare quite well with our laboratory results for type B bores. Also, the gravity current speed compares quite well with our laboratory results, as shown in Fig. 9.

(d) *Observations of a supercritical gravity current*

Goff (1975, 1976) measured 20 thunderstorm outflows as they passed the instrumented tower described in the previous subsection. Among these, we have selected one in which an outflow was observed to advance into a clearly defined ground-based temperature inversion. This event occurred on 27 May 1972 and is depicted in Fig. 9 of Goff (1976).

We have constructed the idealized two-layer model of this event, shown in Fig. 14(d), from the time histories of the temperature and pressure measurements at the tower. The diagram shows a 1000-m-deep gravity current (with density ratio $\alpha = 2.3$) advancing at the rate of 19 m/s into a shallow 200-m lower layer of dense fluid. We estimated the depth of the cold gravity current (which was well above the top of the tower) from the 3 mb pressure increase at the ground. There is no evidence of a bore of any type propagating on the inversion layer in front of the gravity current.

In this case, with $D_0 = 5.0$ and $F_0 = 5.0$, we would not expect, based on our laboratory experiments, an upstream propagating bore to be present. In Fig. 9, this gravity current would be plotted in the region labelled *supercritical or partial blocking* (although the point does not appear in the plot because it lies outside the range shown in the figure), and in all our laboratory experiments in this region of the parameter space we observed only supercritical gravity currents.

(e) *Observations of an intrusion*

The structure of the head of an intrusive gravity current advancing into a two-layer fluid in the laboratory has been described by Britter and Simpson (1981). Intrusions in the atmosphere have been observed to be formed by sea-breeze fronts and thunderstorm outflows. Bedard and Sanders (1978) observed on 27 September 1977, using an acoustic sounder, radar and a dense array of surface sensors at Dulles Airport in Washington D.C., what appears to be an early stage in the formation of a bore by an intrusion resulting from a thunderstorm outflow.

Our two-layer idealization of this event is shown in Fig. 14(e). The figure shows an intrusion (with density ratio $\alpha = -0.35$) propagating at 12.8 m/s along the top of a dense lower layer of depth 300 m. Temperature profiles confirmed the existence of an intrusive form having a wave at the front with a wavelength of about 5 km. From pressure changes at the ground a height of 700 m could be deduced for the gravity current.

These observations are consistent with the structure expected in the early stages of the generation of a bore with a strength of 2.3. This strength identifies the bore as in our type B category. However, the bore is apparently in the very early stages of development and it is difficult to distinguish the bore speed from the speed of the intrusion. We have plotted the speed shown in Fig. 14(e) as the intrusion speed in Fig. 9, where it is seen to compare well with our laboratory observations of intrusions. We have plotted also the wavelength of this bore on the graph in Fig. 5, although the wavelength may well be in a state of change at this very early stage in the bore's development.

6. DISCUSSION AND CONCLUSIONS

We have presented evidence from laboratory experiments that gravity currents can produce internal bores on the interface of a two-layer fluid. In the case when the upper layer is very much deeper than the lower layer, our results show that the hydraulic theory for two-layer flow over a streamlined obstacle of finite length gives a reasonable qualitative estimate of the types of bores generated by gravity currents. However, quantitatively the hydraulic theory does not provide an accurate picture of the structure of the bore as a function of its strength.

We have presented a rule of thumb for what structure the bore has as a function of its strength. When $1 < h_1/h_0 < 2$, the bore has a smooth undular form, when $2 < h_1/h_0 < 4$, the bore is undular but some mixing, due to shear instability, occurs on the downstream face of the leading undulation, and when $h_1/h_0 > 4$, the bore appears like a gravity current. When $h_1/h_0 < 2$ the speed of the bore as a function of h_1/h_0 is well predicted by non-mixing bore theory, but when $h_1/h_0 > 2$ gravity current theory better predicts the speed. The values of h_1/h_0 that distinguish between the different types of bores are probably a function of the ratio of the lower layer depth to the total depth of the fluid. But for small values of this ratio we believe that these distinguishing values do not vary much.

A conclusion of some significance is that it is apparently impossible for a gravity current to block completely the flow in the lower layer, as has been suggested by some previous observers of atmospheric bores. Figure 9 in Tepper (1950), for example, suggests that the lower layer is completely blocked by a gravity current. Since the speed of the gravity current increases with the height of the current head, it is not possible to produce a current that has the height and slow speed required to block the flow. Our efforts to do this by reducing the density difference between the current and the surrounding fluid always resulted in producing an intrusion, a current that moved along the interface between the two ambient fluids, instead of an upstream blocked flow driven by a gravity current travelling along the bottom of the tank.

Somewhat to our surprise, we found that the energy-conserving gravity current theory of Holyer and Huppert (1980), as extended by Crook (1983), fairly accurately predicted the strength and speed of type A bores generated by gravity currents in our two-layer experiments.

We have presented also analyses of several atmospheric observations of internal bores at different stages of development that were generated by some type of gravity current and showed that the atmospheric data compare favourably with our laboratory measurements, although our experiments approximate the atmosphere as a two-layer fluid. To be sure, the atmosphere in general is more complicated than our simple two-layer model and the effects of such complicating factors as stratification in the upper layer, wind shear and moisture may be significant. But our results at least show that there seems little doubt that both thunderstorm outflows and sea-breeze fronts can generate internal bores in stable layers and it is hoped the model we have presented here may point the way to a series of future investigations into the early stages of bore formation in the atmosphere.

ACKNOWLEDGMENTS

We thank Andrew Crook and Roger Smith for many helpful comments on an earlier version of this paper. We acknowledge financial support from the Natural Environment Research Council.

REFERENCES

- Baines, P. G. 1984 A unified description of two-layer flow over topography. *J. Fluid Mech.*, **146**, 127–167
- 1987 Upstream blocking and airflow over mountains. *Ann. Rev. Fluid Mech.*, **19**, 75–97
- Baines, P. G. and Davies, P. A. 1980 Laboratory studies of topographic effects in rotating and/or stratified fluids. Pp. 233–299 in *Orographic effects in planetary flows*, GARP Publ. No. 23
- Bedard, A. J. and Saunders, M. J. 1978 Thunderstorm-related wind shear detected at Dulles international airport. Pp. 347–352 in *Proceedings conference on weather forecasting and analysis and aviation meteorology*. American Meteorological Society, 16–19 Oct., Silver Spring, MD.
- Benjamin, T. B. 1968 Gravity currents and related phenomena. *J. Fluid Mech.*, **31**, 209–248
- Benjamin, T. B. and Lighthill, M. J. 1954 On cnoidal waves and bores. *Proc. R. Soc. Lond.*, **A224**, 448–460
- Binnie, A. M. and Orkney, J. C. 1955 Experiments on the flow of water from a reservoir through an open channel: II. The formation of hydraulic jumps. *ibid.*, **A230**, 237–246
- Britter, R. E. and Simpson, J. E. 1978 Experiments on the dynamics of a gravity current head. *J. Fluid Mech.*, **88**, 223–240
- 1981 A note on the structure of the head of an intrusive gravity current. *ibid.*, **112**, 459–466
- Clarke, R. H. 1965 Horizontal mesoscale vortices in the atmosphere. *Aust. Meteorol. Mag.*, **50**, 1–25
- Clarke, R. H., Smith, R. K. and Reid, D. G. 1981 The Morning Glory of the Gulf of Carpentaria: an atmospheric undular bore. *Mon. Weather Rev.*, **109**, 1726–1750
- Crook, N. A. 1983 The formation of the Morning Glory. Pp. 349–353 in *Mesoscale meteorology—theories, observations and models*. Lilly, D. K. and Gal-Chen, T. (Eds.), D. Reidel
- 1984 'A numerical and analytical study of atmospheric undular bores'. Ph.D. thesis, University of London
- 1986 The effect of ambient stratification and moisture on the motion of atmospheric undular bores. *J. Atmos. Sci.*, **43**, 171–181
- 1988 Trapping of low-level internal gravity waves. *ibid.*, **45**, 1533–1541
- Crook, N. A. and Miller, M. J. 1985 A numerical and analytical study of atmospheric undular bores. *Q. J. R. Meteorol. Soc.*, **111**, 225–242
- Durran, D. R. 1986 Another look at downslope windstorms. Part I: On the development of analogs to supercritical flow in an infinitely deep, continuously stratified fluid. *J. Atmos. Sci.*, **43**, 2527–2543
- Goff, R. C. 1975 'Thunderstorm-outflow kinematics and dynamics'. NOAA Tech. Memo ERLTH-NSSL-75
- 1976 Vertical structure of thunderstorm outflows. *Mon. Weather Rev.*, **104**, 1429–1440
- Haase, S. and Smith, R. K. 1984 Morning Glory wave clouds in Oklahoma: a case study. *ibid.*, **112**, 2078–2089
- Holyer, J. Y. and Huppert, H. E. 1980 Gravity currents entering a two-layer fluid. *J. Fluid Mech.*, **100**, 739–767
- Houghton, D. D. and Kasahara, A. 1968 Nonlinear shallow fluid flow over an isolated ridge. *Commun. Pure Appl. Math.*, **21**, 1–23
- Huppert, H. E. and Simpson, J. E. 1980 The slumping of gravity currents. *J. Fluid Mech.*, **99**, 785–799
- Long, R. R. 1954 Some aspects of the flow of stratified fluids, II. Experiments with a two-fluid system. *Tellus*, **6**, 97–115
- 1970 Blocking effects in flow over obstacles. *ibid.*, **22**, 471–480
- 1972 Finite amplitude disturbances in the flow of inviscid rotating and stratified fluids over obstacles. *Ann. Rev. Fluid Mech.*, **4**, 69–92
- Marks, J. 1974 'Acoustic radar investigations of boundary layer phenomena'. NASA Rpt. CR-2432
- Maxworthy, T. 1980 On the formation of nonlinear internal waves from the gravitational collapse of mixed regions in two and three dimensions. *J. Fluid Mech.*, **96**, 47–64

- | | | |
|---|------|--|
| Pratt, L. J. | 1983 | A note on nonlinear flow over obstacles. <i>Geophys. Astrophys. Fluid Dyn.</i> , 24 , 63–68 |
| Robin, A. G. | 1978 | Roll cloud over Spencer Gulf. <i>Aust. Meteorol. Mag.</i> , 26 , 125 |
| Rottman, J. W. and Simpson, J. E. | 1983 | Gravity currents produced by instantaneous releases of a heavy fluid in a rectangular channel. <i>J. Fluid Mech.</i> , 135 , 95–110 |
| Shreffler, J. H. and Binkowski, F. S. | 1981 | Observations of pressure jump lines in the Midwest, 10–12 August 1976. <i>Mon. Weather Rev.</i> , 109 , 1713–1725 |
| Simpson, J. E. | 1982 | Gravity currents in the laboratory, atmosphere and ocean. <i>Ann. Rev. Fluid Mech.</i> , 14 , 213–234 |
| | 1987 | <i>Gravity currents in the environment and the laboratory</i> . Ellis Horwood |
| Simpson, J. E., Mansfield, D. A. and Milford, J. R. | 1977 | Inland penetration of sea-breeze fronts. <i>Q. J. R. Meteorol. Soc.</i> , 103 , 46–76 |
| Smith, R. K. | 1986 | Evening Glory wave-cloud lines in northwestern Australia. <i>Aust. Meteorol. Mag.</i> , 34 , 27–33 |
| Smith, R. K. and Goodfield, J. | 1981 | The 1979 Morning Glory expedition. <i>Weather</i> , 36 , 130–136 |
| Smith, R. K., Crook, N. and Roff, G. | 1982 | The Morning Glory: an extraordinary atmospheric undular bore. <i>Q. J. R. Meteorol. Soc.</i> , 108 , 937–956 |
| Tepper, M. | 1950 | A proposed mechanism of squall lines—the pressure jump line. <i>J. Meteorol.</i> , 7 , 21–29 |
| Wood, I. R. and Simpson, J. E. | 1984 | Jumps in layered miscible fluids. <i>J. Fluid Mech.</i> , 140 , 329–342 |